Food Control 110 (2020) 107029

Contents lists available at ScienceDirect

Food Control

journal homepage: www.elsevier.com/locate/foodcont

Tandem mass tag-based quantitative proteomics reveals the regulators in biofilm formation and biofilm control of *Bacillus licheniformis*

Ni Wang[a], Faizan Ahmed Sadiq[b], Shanshan Li[a], Guoqing He[a,*], Lei Yuan[a,c,**]

[a] College of Biosystems Engineering and Food Science, Zhejiang University, Hangzhou, 310058, China
[b] School of Food Science and Technology, Jiangnan University, Wuxi, 214122, China
[c] College of Food Science and Engineering, Yangzhou University, Yangzhou, 225127, China

ARTICLE INFO

Keywords:
Bacillus licheniformis
Biofilm formation
Biofilm control
Quantitative proteomics
Regulator

ABSTRACT

Regulatory mechanisms of *Bacillus licheniformis* biofilm formation and biofilm control are desired to be explored as it is a major contaminant with strong spoilage capacity in the dairy industry. In this study, tandem mass tag-based quantitative proteomics was employed to compare the expression profiles between biofilm cells and planktonic cells of *B. licheniformis*. Matrix production and sporulation, bacterial chemotaxis, flagellar assembly and two-component system played important roles on biofilm formation by *B. licheniformis*. Significant up-regulation proteins Spo0F and KapB, as well as down-regulation proteins MotB, FliG and FliK are the key regulators for biofilm prevention by *Lactobacillus plantarum*. The proteomics profiles provide novel insights into the biofilm formation and control of *B. licheniformis*.

1. Introduction

Bacillus licheniformis is a rod-shaped gram-positive spore forming bacterium, which is a facultative aerobe and can grow at various temperatures ranging from 37 °C to 55 °C, thus termed facultative thermophile. This bacterium has been isolated as a major microbial contaminant in milk powder manufactures in China, Uruguayan, Ireland, New Zealand, USA, Australia and many other countries (Reginensi et al., 2011; Ruckert, Ronimus, & Morgan, 2004; Sadiq et al., 2016b; Zou & Liu, 2018). *B. licheniformis* is considered as a common soil bacterium which is widespread in environment. Surveys on its possible contamination routes reported that soil and farm environments, including animal feed, manure, bedding, are preliminary routes of its entry into raw milk (Crielly, Logan, & Anderton, 1994). Many isolates of *B. licheniformis* was reported to potentially cause dairy spoilage in the dairy industry, due to their ability to produce proteases, lipases, and β-galactosidases (Sadiq et al., 2016a). In addition, the same research reported the ability of its spores to survive the thermal treatment of 115 °C for 30 min. The ability of this bacterium to adhere and form biofilm on stainless steel during dairy manufacture on various surfaces including pipelines, plate heat exchanges and evaporators, further exacerbates the issues to the dairy industry (Bremer, Fillery, & McQuillan, 2006; Sadiq et al., 2017). Bacteria embedded in the matrix of extracellular polymeric substances (EPS) are more resistant to cleaning and disinfection regimes than the planktonic cells, making the complete removal of the bacteria an intractable problem (Bridier, Briandet, Thomas, & Dubois-Brissonnet, 2011; Maes et al., 2019; Yuan et al., 2019).

In order to understand the nature of bacterial biofilms, it is indispensable to have knowledge about the molecular determinants of biofilm formation in a bacterial species. Until now, an appreciable number of studies have focused on the molecular determinants of biofilm formation by bacteria of environmental and medical importance. For instance, mechanistic insights into biofilm formation have been provided for *Escherichia coli* (Yang, Wang, He, & Tran, 2018), *Enterococcus faecalis* (Suriyanarayanan et al., 2018), *Listeria monocytogenes* (Huang et al., 2018), *Salmonella* (Sarjit & Dykes, 2017), and *Gardnerella vaginalis* (Castro et al., 2017). The results of these studies have concluded that quorum sensing (QS) plays an important role in biofilm development in many bacterial species (Maddela et al., 2019; Yuan, Sadiq, Burmolle, Liu, & He, 2018). Gram-negative bacteria, such as *E. coli* (Cui, Chen, Liu, Zhou, & Liu, 2019; Yin et al., 2019) and *Pseudomonas aeruginosa* (Maddela et al., 2019; Toyofuku et al., 2008), mostly carry out cell-to-cell communication by N-acylhomoserine lactones (AHLs) signal molecules. Gram-positive bacteria, such as *Staphylococcus aureus* (Karathanasi et al., 2018; Vasquez, Tal-Gan, Cornilescu, Tyler, & Blackwell, 2017), have a more complex QS process based on two-component system with different auto inducer peptides (AIPs)

* Corresponding author. College of Biosystems Engineering and Food Science, Zhejiang University, 866 Yuhangtang Road, Hangzhou, 310058, China.
** Corresponding author. College of Food Science and Engineering, Yangzhou University, 196 Huayang West Road, Yangzhou, 225127, China.
E-mail addresses: gqhe@zju.edu.cn (G. He), leiyuan0926@163.com (L. Yuan).

https://doi.org/10.1016/j.foodcont.2019.107029
Received 9 August 2019; Received in revised form 28 November 2019; Accepted 30 November 2019
Available online 02 December 2019
0956-7135/

depending on the strains. Because of the specificity of AIPs, mechanisms of biofilm formation by many gram-positive bacteria are still not well understood. It is reported that biofilm cells of *Streptococcus mutants*, once treated with cell free supernatant (CFS) of a *Lactobacillus* sp., showed reduced expression of genes related to exopolysaccharide production, acid tolerance and QS (Wasfi, Abd El-Rahman, Zafer, & Ashour, 2018). Merino, Trejo, De Antoni, and Golowczyc (2019) also found that the biofilm formation of *Salmonella* sp. isolates from poultry were inhibited by *Lactobacillus*.

Biofilms formed by *B. licheniformis* pose an important threat to the dairy industries throughout the world, and a complete understanding of the mechanism of its biofilm formation is needed. Our group recently reported the role of *Lactobacillus plantarum* metabolites in controlling biofilms formed by *B. licheniformis* strains (Wang, Yuan, Sadiq, & He, 2019), however, the inhibition mechanism is still unknown. In this study, regulators of biofilm formation were determined by comparing the protein expression of biofilm and planktonic cells of *B. licheniformis*. In addition, regulators involved in controlling biofilms by *B. licheniformis* in the presence of *L. plantarum* metabolites are also determined. These results extend the knowledge on the mechanism of biofilm formation and biofilm control of *B. licheniformis* by providing previously unreported mechanistic insights.

2. Material and methods

2.1. Strains and growth conditions

B. licheniformis was previously isolated from Chinese milk powder products (Sadiq et al., 2016b), with an alignment identity of 99.66% to *B. licheniformis* ATCC 14580. *L. plantarum* was isolated from Chinese traditional sourdough (Liu et al., 2016).

Overnight culture of *L. plantarum* was centrifuged at 6000 rpm for 10 min and filtered with 0.22-μm polyethersulfone membrane (PES, Merk, Germany), then CFS was mixed with tryptic soy broth (TSB, Difco, USA) for *B. licheniformis* cultivation. *B. licheniformis* culture was diluted with TSB to the concentration of 10^4 CFU/mL for incubation. Two experimental groups, biofilm formation and biofilm intervention, were grown in 24-well cell culture plates (Costar, Corning, USA). Experimental groups of biofilm formation (samples of bfm-1, bfm-2, bfm-3, plkt-1, plkt-2, plkt-3) contained 120 μL of *B. licheniformis*, 400 μL of phosphate buffer saline (PBS, pH 6.5), and 1480 μL of TSB in each well. Experimental groups of biofilm intervention (samples of plktlps-1, plktlps-2, plktlps-3) contained 120 μL of *B. licheniformis*, 680 μL of *L. plantarum* CFS, 400 μL of PBS (pH 6.5) and 800 μL of TSB in each well. Each group had 48 replicate wells, and was incubated at 55 °C for 24 h.

2.2. Sample preparations of biofilm cells and planktonic cells

Samples of bfm-1, bfm-2, bfm-3 were collected from the biofilm cells of *B. licheniformis* in the experimental groups of biofilm formation, and samples of plkt-1, plkt-2, plkt-3 were harvested from the planktonic cells in this group. There were very few biofilm cells in the experimental group of biofilm intervention by *L. plantarum* CFS since the biofilms were inhibited, and samples of plktlps-1, plktlps-2, plktlps-3 were harvested from the planktonic cells in this group. Bacterial cells from the 9 samples were centrifuged at 6000 rpm for 10 min at 4 °C separately, and the precipitates were washed three times with PBS. Then the cells were frozen immediately with liquid nitrogen and stored at −80 °C.

2.3. Protein extraction and digestion

Both the biofilm cells and planktonic cells, 9 samples in total, were resuspended and lysed on ice in 200 μL buffer (pH 8.0) containing 4% sodium dodecyl sulfate (Sigma, USA), 100 mM dithiothreitol (Sigma, USA), and 150 mM Tris-HCl (Sigma, USA). The bacterial cells were disrupted using a homogenizer and boiled for 5 min, then ultrasonicated and boiled again for another 5 min. After that, the undissolved debris were removed by centrifugation for 15 min at 16000 rpm, and the proteins in the supernatant were collected. Protein concentrations were estimated with a Bicinchoninic Acid Protein Assay Kit (Bio-Rad, USA).

The amount of 300 μg proteins of each sample was digested according to the filter-aided sample preparation (FASP) procedure (Wisniewski, Zougman, Nagaraj, & Mann, 2009). Briefly, 200 μL of uric acid (UA) buffer (pH 8.0) containing 8 M urea (Sigma, USA) and 150 mM Tris-HCl, was added into each sample, and then ultra-filtrated with a molecular weight cutoff of 10 kDa. After that, 100 μL of 50 mM iodoacetamide (Sigma, USA) in UA buffer was mixed to the protein samples and incubated for 20 min in darkness, followed by washing with 100 μL of UA buffer three times and then 100 μL of 25 mM NH_4HCO_3 (Sigma, USA) twice. Subsequently, the protein suspension was digested with 4 μg of trypsin (Promega, USA) in 40 μL of 25 mM NH_4HCO_3 at 37 °C for 16 h, then digested protein samples were centrifuged at 16000 rpm for 10 min and collected.

2.4. Tandem mass tag (TMT) labeling of peptides and high pH reverse-phase peptide (HPRP) fractionation

Peptides were labeled with TMT10plex Isobaric Label Reagent Set (Thermo Fisher Scientific, USA) according to the manufacturer's instructions at room temperature for 1 h before quenching the reaction with 5% hydroxylamine for 15 min. Among the 9 samples, bfm-1 was labeled with 126, bfm-2 with 127N, bfm-3 with 127C. Samples of plkt-1 was labeled with 128N, plkt-2 with 128C, plkt-3 with 129N. Samples of plktlps-1 was labeled with 129C, plktlps-2 with 130N, plktlps-3 with 130C. After labelling, the samples were combined and desalted.

TMT-labeled peptide mixture was fractionated using a Pierce HPRP Fractionation Kit (Thermo Fisher Scientific, USA) according to the manufacturer's instructions. A total of 30 fractions were collected, then merged into 15 fractions and lyophilized before liquid chromatography-mass spectrometry/mass spectrometry (LC-MS/MS) analysis.

2.5. LC-MS/MS analysis of the peptides

A total of 15 fractions of the peptide mixtures were dissolved in 0.1% formic acid separately and prepared for LC-MS/MS Analysis. LC-MS/MS was performed on a Q-Exactive Plus mass spectrometer (Thermo Fisher Scientific, USA) that was coupled to Easy-nLC 1200 system, nano HPLC. Peptides from each fraction were loaded onto an Acclaim PepMap100 Nano Trap Column (2 cm × 100 μm, 5 μm, C18, Thermo Fisher Scientific, USA), then onto an EASY-Spray Column (75 μm × 120 mm, 3 μm, C18, Thermo Fisher Scientific, USA). Mobile phase A consisted of 0.1% (V/V, the same below) formic acid in water, and mobile phase B consisted of 0.1% formic acid and 98% acetonitrile in water at a flow rate of 300 nL/min. The gradient elution of mobile phase B was set as follows: from 4% to 7% for 0–2 min, from 7% to 20% for 2–67 min, from 20% to 35% for 67–79 min, from 30% to 90% for 79–81 min, maintaining at 90% for 81–90 min.

MS data were acquired using a data-dependent mode. Precursor ions were selected across a mass range of 300–1800 *m/z*. A maximum of 20 most abundant precursor ions per cycle from each MS spectra were selected for HCD fragmentation. Determination of the target value was based on predictive automatic gain control (AGC). The AGC target value of 1e6, a resolution of 70000 at *m/z* 200, and maximum injection time of 50 ms were set in MS scan. A target AGC value of 1e5, and a resolution of 35000 at *m/z* 200, and maximum injection time of 50 ms were set in MS/MS scan. Dynamic exclusion duration was 30 s, and normalized collision energy was 35.

2.6. Protein identification and quantification

The raw files of LC-MS/MS results were imported into MaxQuant software (version 1.6.0.16) for protein identification against the database Uniprot-Bacillus-licheniformis_4164_20190201.fasta (https://www.uniprot.org/uniprot/?query=taxonomy:279010). The parameters were set as follows: sample type, reporter ion MS2; isobaric labels, TMT 10plex; enzyme, trypsin; reporter mass tolerance, 0.005 Da; max missed cleavages, 2; main search peptide tolerance, 4.5 ppm; first search peptide tolerance, 20 ppm; MS/MS tolerance, 20 ppm; fixed modifications, carbamidomethyl (C); variable modifications, oxidation (M) and acetyl (protein N-term); database pattern, target-reverse; peptide-to-spectrum match (PSM) false discovery rate (FDR) ≤ 0.01; protein FDR ≤ 0.01. Razor and unique peptides were used for quantification. The minimum of six amino acids and one unique peptide were required for each protein.

2.7. Bioinformatics analysis of differentially expressed proteins

Perseus software, Microsoft Excel and R statistical computing software were used for bioinformatics analysis (Tyanova et al., 2016). Differentially expressed proteins were screened with a cutoff of fold-change > 1.20 or < 0.83, and P-value < 0.05. The annotated functions of the proteins were analyzed by the Gene Ontology (GO) (Ashburner et al., 2000) annotation software (http://david.abcc.ncifcrf.gov/home.jsp). Hierarchical clustering of the identified proteins was conducted with Cluster 3.0 software originally developed by Michael Eisen. Pathway analysis of the identified proteins was performed via the Kyoto Encyclopedia of Genes and Genomes (KEGG) (Kanehisa, Goto, Sato, Furumichi, & Tanabe, 2012) pathway database (http://www.genome.jp/kegg). GO and KEGG enrichment analyses were carried out with the Fisher's exact test, and FDR correction for multiple testing was also performed. Construction of protein-protein interaction (PPI) networks were conducted using the STRING database (http://string-db.org/) with the cytoscape software. Venn's diagram was processed using Venny 2.1.0 by Oliveros, J. C. (http://bioinfogp.cnb.csic.es/tools/venny/index.html).

2.8. Parallel reaction monitoring (PRM) analysis of the target proteins

To verify the protein expressions obtained by TMT analysis, the expressions of eight selected proteins were further quantified by LC-PRM/MS analysis. Signature peptides for the target proteins were defined based on shotgun analysis. Only unique peptide sequences were selected for the PRM assays. Briefly, 200 μg of the proteins from each sample were extracted and digested according to the TMT protocol. The obtained peptide mixtures (2 μg for each sample) were introduced into Easy-nLC 1200 system, nano HPLC (Thermo Fisher Scientific, USA). Mobile phase A consisted of 0.1% formic acid in water, and mobile phase B consisted of 0.1% formic acid and 95% acetonitrile in water at a flow rate of 300 nL/min. Q-Exactive Plus mass spectrometer that was coupled to peptides from each fraction was loaded onto an Acclaim PepMap100 Nano Trap Column (2 cm × 100 μm, 5 μm, C18, Thermo Fisher Scientific, USA). The gradient elution of mobile phase B was set as follows: from 2% to 5% for 0–5 min, from 5% to 23% for 5–45 min, from 23% to 40% for 45–50 min, from 40% to 100% for 50–52 min, maintaining at 100% for 52–60 min. Precursor ions were selected across a mass range of 350–1500 *m/z* with a resolution of 70000 at *m/z* 200. The AGC target value of 3e6, and maximum injection time of 200 ms were set in MS scan. A target AGC value of 3e6, a resolution of 35000 at *m/z* 200, and maximum injection time of 100 ms in HCD mode were set in MS/MS scan. Isolation window was 2.0 Th, and normalized collision energy was 27. The raw data obtained were then analyzed with Skyline 4.1 software for PRM data processing.

2.9. Statistical analysis

All experiments in this study were conducted in triplicate. In order to detect significant differences ($P < 0.05$), all data were subjected to analysis of variance (ANOVA) with Duncan's multiple range test using SPSS statistical software (version 22, IBM, USA).

3. Results

3.1. Differently expressed proteins identified by TMT profiling of B. licheniformis

A total of 2048 quantified proteins listed in Table S1 were obtained in the TMT analysis. In the comparison of the biofilm cells and planktonic cells (bfm/plkt), 491 proteins were detected to be differently expressed, among which, 238 proteins were up-regulated and 253 proteins were down-regulated. In the comparison of the biofilm cells and planktonic cells inhibited by *L. plantarum* CFS (bfm/plktlps), 890 proteins were detected to be differently expressed, among which, 453 proteins were up-regulated and 437 proteins were down-regulated. Differently expressed proteins in the two comparisons were also displayed by volcano plots (Fig. S1) and hierarchical clustering (Fig. S2).

Venn's diagram showed the common elements among these four parts (Fig. 1). A number of 221 proteins were significantly up-regulated in both of bfm/plkt and bfm/plktlps. For instance, putative 8-amino-7-oxononanoate synthase encoded by *bioF*, which is involved in the pathway of biotin biosynthesis, is a part of cofactor biosynthesis. Superoxide dismutase, encoded by *sodF*, helps in mental iron binding. Spore coat protein (outer), encoded by *cotM*, is related to viral capsid. Extracellular serine protease, encoded by *vpr*, has serine-type endopeptidase activity. Secreted biofilm formation protein, encoded by *yqxM*, helps in cellular component of bacterial biofilm matrix.

A number of 223 proteins were significantly down-regulated in both of bfm/plkt and bfm/plktlps. For instance, anaerobic ribonucleoside-triphosphate reductase-activating protein, encoded by BL02467, is responsible for activation of anaerobic ribonucleoside-triphosphate reductase under anaerobic conditions by generation of an organic free radical, using S-adenosylmethionine and reduced flavodoxin as co-substrates to produce 5′-deoxy-adenosine. Integral membrane protein encoded by *yceF*, belonging to TerC family, is the integral component of membrane. Flagellin, encoded by *hag*, is the subunit protein which polymerizes to form the filaments of bacterial flagella.

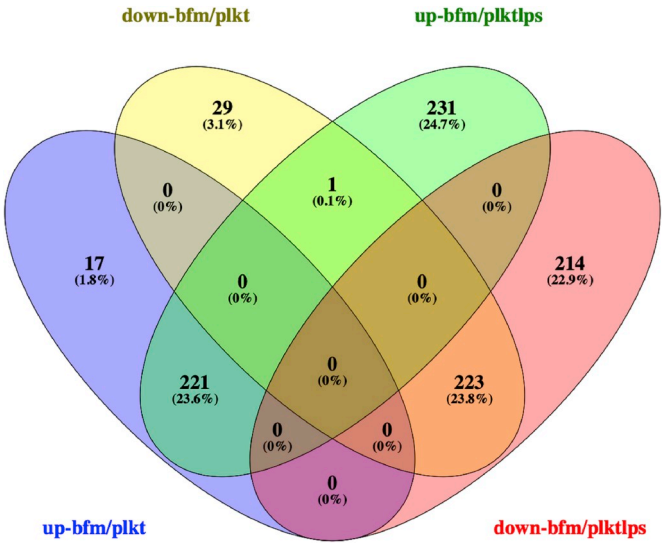

Fig. 1. Venn's diagram of common elements among the four parts: up-regulated proteins of bfm/plkt, dowm-regulated proteins of bfm/plkt, up-regulated proteins of bfm/plktlps, dowm-regulated proteins of bfm/plktlps.

Apart from the common up-regulated proteins, another 231 proteins were significantly up-regulated in the comparison of bfm/plktlps. For example, putative serine protease, encoded by *yyxA*, has serine-type endopeptidase activity. Apart from the common down-regulated proteins, another 214 proteins were significantly down-regulated in bfm/plktlps. For example, phosphoribosylglycinamide formyltransferase, encoded by *purN*, catalyzes the transfer of a formyl group from 10-formyltetrahydrofolate to 5-phospho-ribosyl-glycinamide, producing 5-phospho-ribosyl-N-formylglycinamide and tetrahydrofolate. Apart from the common up-regulated proteins, another 17 proteins were significantly up-regulated only in comparison of bfm/plkt. For example, spore coat protein (insoluble fraction), encoded by *cotZ*, is related to viral capsid. Apart from the common down-regulated proteins, another 29 proteins were significantly down-regulated in bfm/plkt. For example, ATP-dependent 6-phosphofructokinase, encoded by *pfkA*, catalyzes the phosphorylation of D-fructose 6-phosphate to fructose 1,6-bisphosphate by ATP, the first committing step of glycolysis.

3.2. GO enrichment analysis of differently expressed proteins in biofilm formation and biofilm control of B. licheniformis

GO enrichment analysis of differently expressed proteins based on GO level 4 was performed. In the categories of biological process (BP), and cellular component (CC), molecular function (MF), the differently abundant proteins were classified as shown in Fig. 2.

For comparison of bfm/plkt in biological process, the differently abundant proteins distributed in organonitrogen compound metabolic process (22.7%), small molecule metabolic process (19.0%), protein metabolic process (13.6%), organic substance catabolic process (9.1%), single-organism catabolic process (7.4%), carbohydrate metabolic process (7.4%), glycosyl compound metabolic process (6.6%), cellular catabolic process (5.8%), single-organism carbohydrate metabolic process (5.0%), generation of precursor metabolites and energy (3.3%). In cellular component, the differently abundant proteins distributed in cytoplasm (55.6%), intracellular organelle (19.2%), intracellular ribonucleoprotein complex (18.2%), intracellular organelle part (7.1%). None of the differently abundant proteins in molecular function were obtained in bfm/plkt.

For the comparison of bfm/plktlps in BP, the differently abundant proteins distributed in organonitrogen compound metabolic process (20.6%), small molecule metabolic process (18.1%), protein metabolic process (11.4%), carbohydrate derivative metabolic process (8.1%), organophosphate metabolic process (7.9%), organic substance catabolic process (6.3%), glycosyl compound metabolic process (5.3%), carbohydrate metabolic process (5.3%), single-organism catabolic process (5.1%), cellular catabolic process (4.9%), single-organism carbohydrate metabolic process (3.7%), organic hydroxy compound metabolic process (2.0%), tricarboxylic acid cycle (0.6%), thioester metabolic process (0.6%). In CC, the differently abundant proteins distributed in cytoplasm (78.4%), intracellular organelle (21.6%). In MF, the differently abundant proteins distributed in nucleoside binding (34.0%), ribonucleotide binding (30.4%), anion binding (29.8%), ligase activity, forming carbon-oxygen bonds (5.8%).

3.3. Pathway enrichment analysis of differently expressed proteins in biofilm formation and biofilm control of B. licheniformis

In comparison of bfm/plkt (Fig. 3A), differently abundant proteins by KEGG analysis mainly participated in microbial metabolism in glycolysis/gluconeogenesis, carbon metabolism, butanoate metabolism, microbial metabolism in diverse environments, bacterial chemotaxis. In bfm/plktlps (Fig. 3B), differently abundant proteins by KEGG analysis mainly participated in geraniol degradation, biosynthesis of antibiotics, pyruvate metabolism, carbon metabolism, propanoate metabolism.

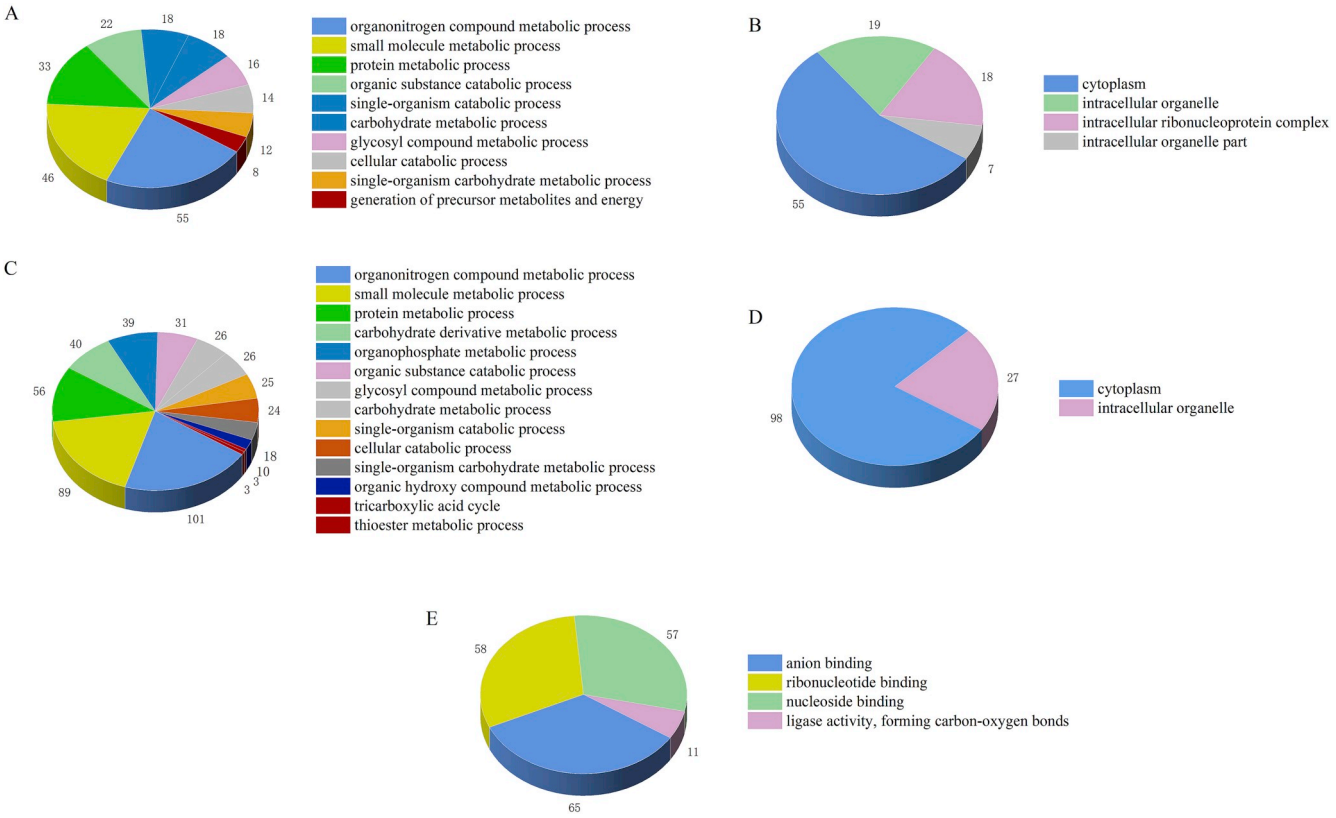

Fig. 2. GO enrichment analysis of differently expressed proteins in the process of biofilm formation and biofilm control of *B. licheniformis*. The number of the proteins of each part was marked besides. (A) biological process analysis for bfm/plkt; (B) cellular component analysis for bfm/plkt; (C) biological process analysis for bfm/plktlps; (D) cellular component analysis for bfm/plktlps; (E) molecular function analysis for bfm/plktlps.

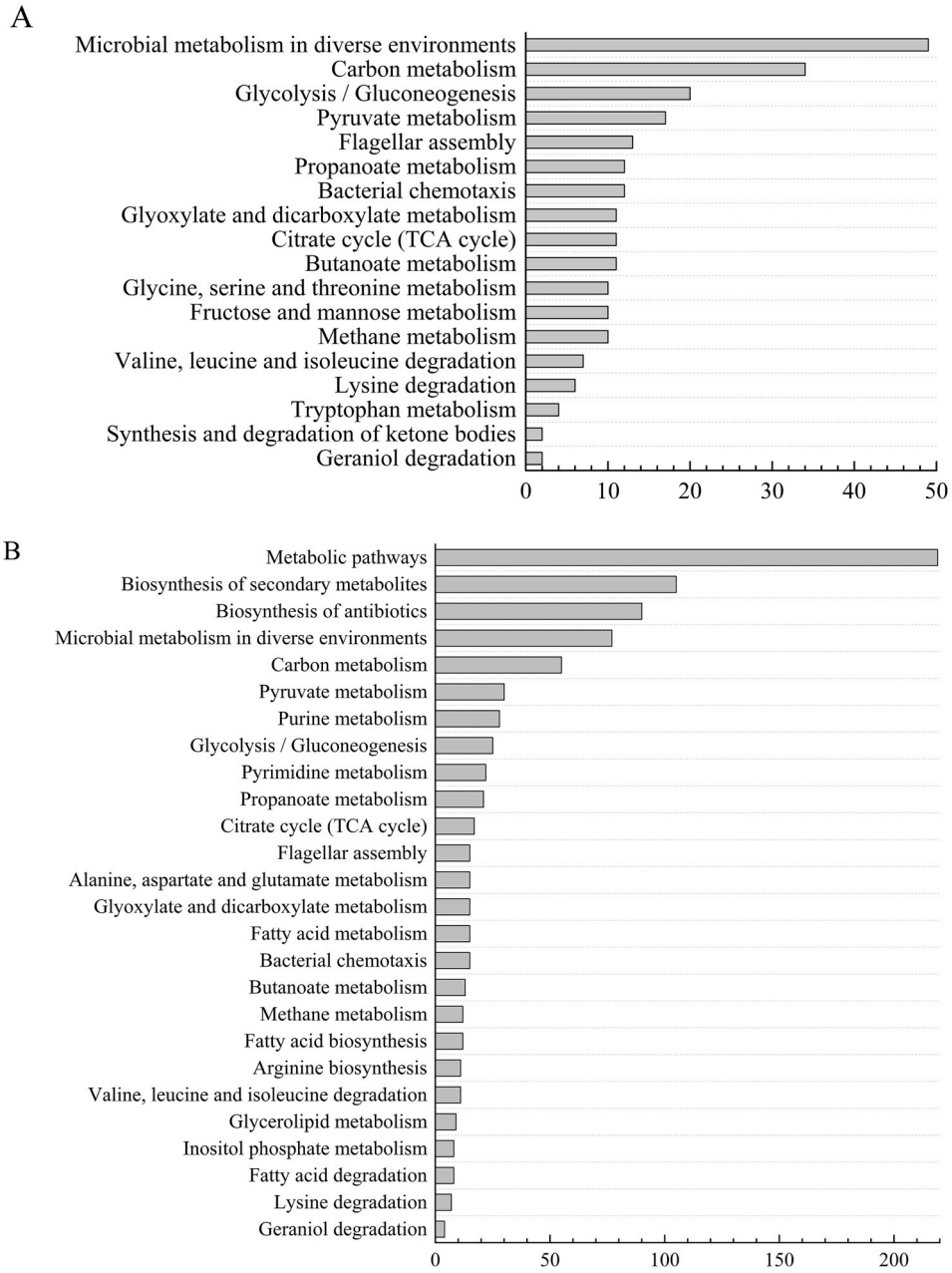

Fig. 3. Pathway enrichment analysis of differently expressed proteins in the process of biofilm formation and biofilm control of *B. licheniformis*. (A) KEGG analysis for bfm/plkt; (B) KEGG analysis for bfm/plktlps.

3.4. PPI network on key pathways in biofilm formation and biofilm control of B. licheniformis

The interaction network of some important differently expressed proteins in bfm/plkt and bfm/plktlps were shown in Fig. 4. PPI network focused on several key pathways of energy metabolism and biofilm formation metabolism, including glycolysis/gluconeogenesis, carbon metabolism, microbial metabolism in diverse environments, bacterial chemotaxis, flagellar assembly, citrate cycle, two-component system, biosynthesis of antibiotics. Biofilm related proteins in pathways of bacterial chemotaxis, flagellar assembly and two-component system, were relatively less associated with others in primary and secondary metabolism. Two-component system presented to be a link between those basic metabolism and biofilm metabolism. In bfm/plktlps comparison, connections to bacterial chemotaxis and flagellar assembly pathways were cut off. Results of biofilm intervention also reflected the important roles of bacterial chemotaxis, flagellar assembly and two-component system on biofilm formation.

3.5. Conformation of TMT data by PRM assay

Eight selected proteins (Q65IH9, Q65CS2, Q65J56, Q65GN5, Q65GG1, Q62PP5, Q65MS5, Q65M10), which had highly significant fold changes in TMT test and were closely related to biofilm formation, were verified by PRM analysis. The quantitative results by PRM analysis were shown in Table 1, and chromatograms used in PRM analysis were provided in Fig. S3. The protein levels in comparisons of bfm/plkt and bfm/plktlps were observed to be up-regulated or down-regulated with the same trend when compared to TMT results.

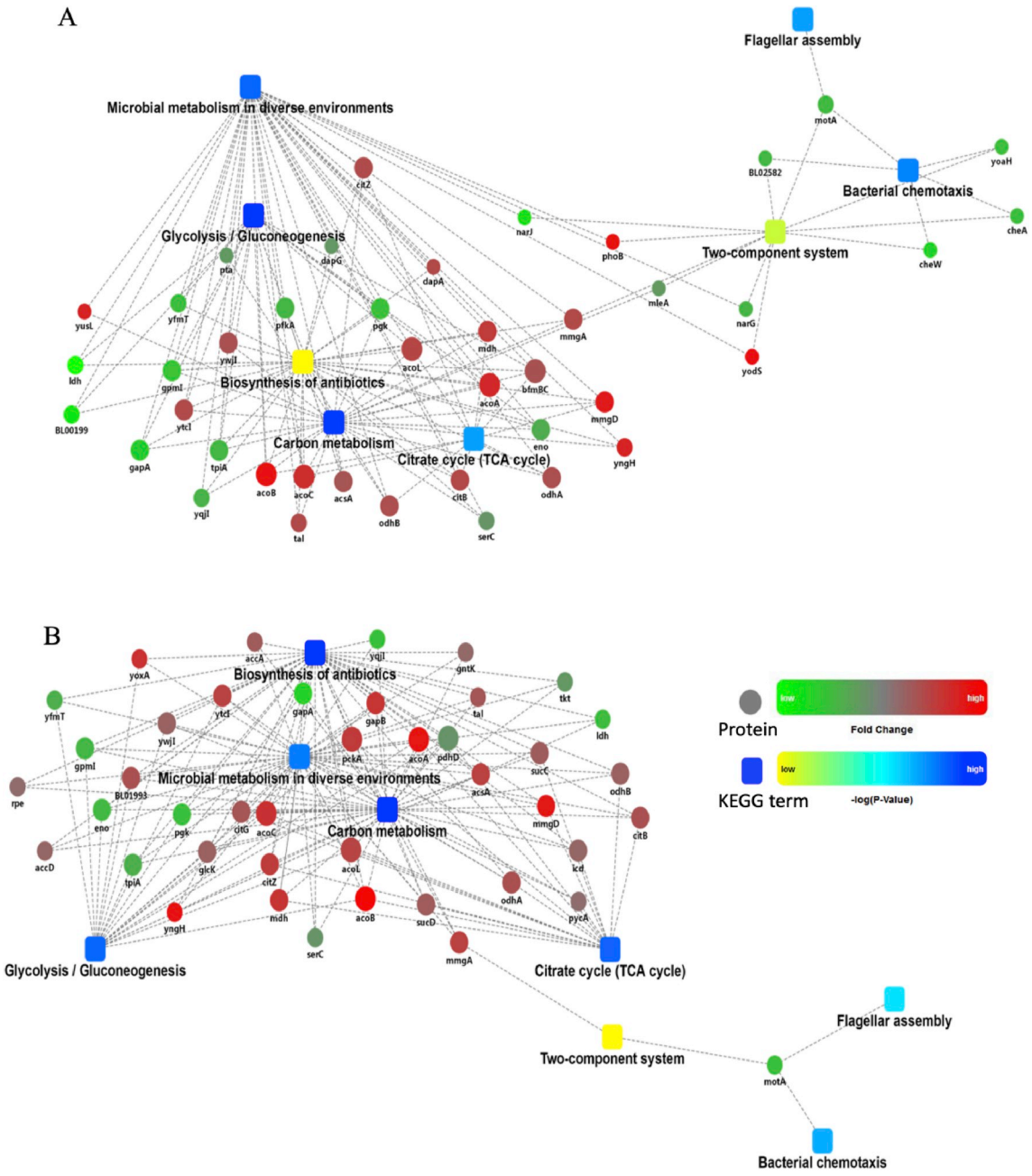

Fig. 4. Interaction network of differently expressed proteins in the process of biofilm formation and biofilm control of *B. licheniformis*. (A) interaction network of bfm/plkt; (B) interaction network of bfm/plktlps.

4. Discussion

Key regulators in biofilm formation and control of *B. licheniformis*, based on the analysis of the numbers and functions of differently expressed proteins, were presented in Fig. 5. The key proteins involved were listed in Table 2.

4.1. Proteins involved in bacterial chemotaxis and cell motility in biofilm formation by B. licheniformis

Biofilm formation is triggered by changes of the environment as the cell density grows. When planktonic cells sense chemical gradients in the environment, such as nutrient deficiency and toxins accumulation, they will adopt more favorable survival strategies. In chemotaxis, events at the receptors control autophosphorylation of the CheA histidine kinase, and the phosphohistidine is the substrate for the response regulator CheY, which catalyzes the transfer of the phosphoryl group to a conserved aspartate. The resulting CheY-P can interact with the switch mechanism in the motor. This interaction causes changes of cell behaviors, such as the direction or speed of rotation of flagella (Ward et al., 2019). *B. licheniformis* uses its flagella to swim and swarm, and its flagella consist of a filament of subunits of the flagellin protein, encoded by the gene *hag*, and a motor subunit that enables the flagellar hook and filament rotation, formed by the proteins MotA and MotB (Voigt et al., 2006). The mode of swimming is influenced by the chemotaxis machinery governed by the two-component system CheA-CheY. Flagellar motor switch proteins, FliG, FliM and FliY, function as a molecular clutch that inhibit flagellar rotation. Changes in chemotaxis and flagella shut off the motility of *B. licheniformis* cells, making it easier for cells to stick together and construct biofilms (Subramanian, Gao, Dann, & Kearns, 2017).

Table 1
Representative protein quantitative confirmation with PRM analysis.

Protein ID	Peptide Sequence	Fold change bfm/plkt	Fold change bfm/plktlps
Q65IH9	TVPIGGHR	3.05	2266.99
Q65CS2	GGQGAQQGGTVR	2.99	2614.03
Q65J56	ANLNAESQGR	3.15	639.82
Q65GN5	YEVDFEELK LNSQLSNPDLIMPGMK	3.47	176.40
Q65GG1	EDGTAIADFSNEFK SGLLSDFQGDVK	2.85	140.59
Q62PP5	DLTLLYR	0.08	0.13
Q65MS5	AAFEQVIVEQLR SETLASLEEK	0.26	0.09
Q65M10	GGGYYVEYR FGAEAVNYAK IVNAAGPWVDR	0.41	0.07

4.2. Proteins involved in matrix production and sporulation in biofilm formation by *B. licheniformis*

The matrix termed EPS is secreted by the non-mobile cells, resulting in pellicles at the air-liquid interface of *B. licheniformis*. Glycosyltransferase is required for EPS synthesis, and inhibition of cell motility occurs independently of the glycosyltransferase activity of the protein. This remarkable mechanism of regulation ensures that cells shut off motility when matrix production occurs to initiate biofilm formation (Blair, Turner, Winkelman, Berg, & Kearns, 2008).

Spo0A pathway plays an important role in biofilm formation, for it participates both sporulation and matrix production. In the two-component system pathway of *B. licheniformis*, Spo0A is phosphorylated with up-regulation of the KinE kinase, cooperating with the other four kinases, KinA, KinB, KinC and KinD. Phosphoryl group is passed to Spo0A directly, or transmitted by Spo0F and Spo0B indirectly, then Spo0A-P regulates both pathways of sporulation and matrix gene expression. It has been reported that serine depletion triggered biofilm induction in *Bacillus subtilis* due to global ribosome pausing on selective serine codons during translation and specifically a decrease in translation of the master biofilm repressor gene *sinR* (Greenwich et al., 2019; Subramaniam et al., 2013). Compared to the well-studied model organism, *B. subtilis*, which promoted the biofilm formation by SlrR-SinI regulator under the control of Spo0A-P (Rey et al., 2004; Vlamakis, Chai, Beauregard, Losick, & Kolter, 2013), however, no evidence showed that differently expressed proteins of *B. licheniformis* was related to the SlrR-SinI regulatory circuit in this study. Unlike gram-negative bacteria, cell communication and biofilm formation of gram-positive bacteria are of more complexity and specificity, even between close species.

Proteins involved in different stages of sporulation (stage 0-VI) were found in both comparisons of bfm/plkt and bfm/plktlps. Due to bacterial growth and changes of the environment, sporulation becomes a survival strategy under the condition of high cell density and nutrient depletion. The cells in the biofilm are under a balance of sporulation, germination and general growth, while spores are released when biofilms are matured. In this process, proteins related to autolysin producing are also activated. It is worth noting that one common element in down-bfm/plkt and up-bfm/plktlps, of which the protein ID is UniProtKB-Q62U05, an uncharacterized protein encoded by BL05210. BL05210 has a combined score of 0.585 with BL01391, which is coded for spore germination B3/GerAC like protein. The GerAA, GerAB, and GerAC proteins of the *B. subtilis* spore are required for the germination response to L-alanine as the sole germinant. Members of GerAC family are thought to be located in the inner spore membrane (Hudson et al., 2001).

4.3. Proteins involved in adaption and survival in biofilm formation by *B. licheniformis*

During the process of biofilm formation, *B. licheniformis* was changing pathways for adaption and survival, especially in nitrogen metabolism, fructose and mannose metabolism, fatty acid metabolism, arginine biosynthesis, lysine biosynthesis. Some up-regulated proteins were detected, such as oligopeptide ABC transporter, ribose ABC transporter, phosphotransferase system, extracellular serine protease, while down-regulated proteins included L-lactate permease, L-lactate dehydrogenase, nitrate reductase, ABC transporter. Changes of these proteins indicate the starving cells adopted the strategy of sporulation due to the high cell density. Without the formation of dormant spores, the cells may need active metabolism to maintain the biofilm state (Ren et al., 2004).

As pellicles at the air-liquid interface got thicker, *B. licheniformis*, a facultative aerobic bacterium, initiated related metabolic pathways under relative anaerobic condition. Anaerobic ribonucleoside-triphosphate reductase-activating protein was significantly down-regulated because planktonic cells beneath the pellicles changed their respiration pathways. Anaerobic ribonucleoside-triphosphate reductase is activated under anaerobic conditions by generation of an organic free radical, using S-adenosylmethionine and reduced flavodoxin as co-substrates to produce 5′-deoxy-adenosine. At the same time, superoxide dismutase (SOD) was significantly up-regulated, especially in bfm/plktlps. SOD has been found correlative to biofilm formation in many species, such as *Salmonella typhimurium* (Wang et al., 2018), *Bacillus cereus* 905 in the

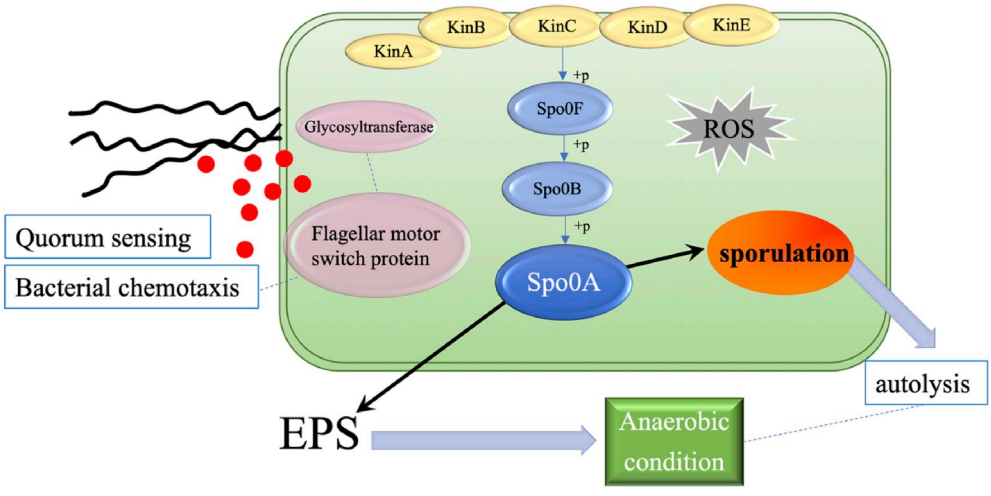

Fig. 5. Schematic diagram of key regulators in biofilm formation and biofilm control of *B. licheniformis*.

Table 2
List of key regulators in biofilm formation and control of *B. licheniformis*.

Protein ID	Fold change		Description	Gene
	bfm/plkt	bfm/plktlps		
Q65HF1	2.229	2.639	Secreted biofilm formation protein	*yqxM*
Q65JM0	0.584	0.468	Flagellar hook protein	*flgE*
Q65JK9	0.556	0.420	Flagellar biosynthesis protein	*flhA*
Q65JK8	0.546	0.356	Flagella-associated protein	*flhF*
Q65EB4	0.585	0.465	Flagellar hook-associated protein 3	*flgL*
Q65E25	0.671	0.598	Flagellar basal body protein	*flhP*
Q65EC0	0.703	0.476	Flagellar hook-associated protein 2	*fliD*
Q65JM8	0.597	0.378	Flagellar M-ring protein	*fliF*
Q65JM7	ns	0.281	Flagellar motor switch protein	*fliG*
A5A676	0.493	ns	Flagellar assembly protein	*fliH*
Q65JM5	0.634	0.549	Flagellar-specific ATP synthase	*fliI*
Q65JM2	0.801	ns	Flagellar protein	*fliK*
Q65JL8	ns	0.461	Flagellar protein	*fliL*
Q65JL7	0.525	0.503	Flagellar motor switch protein	*fliM*
Q65EC1	0.445	0.279	Flagellar secretion chaperone	*fliS*
Q65EC2	0.667	0.461	Flagellar protein	*fliT*
Q65JL6	0.468	0.279	Flagellar motor switch protein	*fliY*
Q65EB9	0.556	0.382	Flagellar protein	*yvyC*
Q65EB8	0.352	0.275	Flagellin	*hag*
Q65KI9	0.540	0.440	Motility protein A	*motA*
Q65KJ0	ns	0.469	Motility protein B	*motB*
Q65ED5	0.783	0.647	Motility/swarming protein	*swrB*
Q65DT9	ns	2.041	Two-component response regulator	*spo0F*
Q65FI0	ns	1.377	Two-component response regulator	*comA*
Q65G90	1.516	2.602	Two-component response regulator	*phoP*
Q65G91	1.368	2.093	Two-component sensor histidine kinase	*phoR*
Q65CY0	0.605	0.738	Two-component response regulator	*yxdJ*
Q65JK5	0.518	0.405	Two-component sensor histidine kinase	*cheA*
Q65JL5	0.668	0.410	Two-component response regulator	*cheY*
Q65KK4	1.309	1.589	Two-component sensor histidine kinase	*kinE*
Q65IH9	2.219	33.136	Superoxide dismutase	*sodF*
Q62PR8	0.536	0.503	Glycosyl transferase family 2	*tuaG*
Q65E82	ns	0.680	Glycosyl transferase family 4	*BL02462*
Q65E99	ns	0.485	Glycosyl transferase family 4	*tuaH*
Q62PP5	0.182	0.210	Anaerobic ribonucleoside-triphosphate reductase-activating protein	*BL02467*
Q65HJ7	1.749	4.877	Stage 0 sporulation protein A	*spo0A*
Q65CN8	0.786	0.755	Stage 0 sporulation protein J	*spo0J*
Q65GL1	1.717	3.441	SpoIIB	*spoIIB*
Q65KZ9	ns	3.916	Stage II sporulation protein SA SpoIISA	*spoIISA*
Q65L00	1.425	2.697	Stage II sporulation protein SB SpoIISB	*spoIISB*
Q62SY0	ns	2.402	SpoIIIAA	*spoIIIAA*
Q65HI2	1.629	3.906	SpoIIIAG	*spoIIIAG*
Q65I19	1.594	5.181	Stage IV sporulation protein A	*spoIVA*
Q65GM1	ns	3.146	SpoIVFA	*spoIVFA*
Q65HU8	ns	1.760	SpoVAD	*spoVAD*
Q65HC9	1.628	2.403	SpoVAFA	*spoVAFA*
Q65J83	ns	1.873	SpoVK	*spoVK*
Q65JE9	ns	2.248	SpoVS	*spoVS*
Q65GK5	1.522	3.256	SpoVID	*spoVID*
Q65GN5	ns	5.933	Morphogenetic protein associated with SpoVID	*safA*
Q65L82	1.988	3.665	SpoVIF	*spoVIF*
Q65E89	ns	0.636	Modifier protein of major autolysin LytC (CWBP76)	*lytB*
Q65E90	0.591	0.461	N-acetylmuramoyl-L-alanine amidase (Major autolysin) (CWBP49)	*lytC*
Q65E77	0.619	0.537	N-acetylglucosaminidase (Major autolysin), Glycoside Hydrolase Family 73	*lytD*

ns = no significance (0.83 ≤ fold change ≤ 1.2 or P ≥ 0.05).

wheat rhizosphere (Gao et al., 2019; Gao, Li, Ding, Chai, & Wang, 2017) and *Pseudomonas putida* MnB1 (Zheng et al., 2018), which may be a primary protective strategy in favor of bacterial adaption and survival.

4.4. Regulators in biofilm control of *B. licheniformis* by *L. plantarum*

Expression changes in the biofilm intervention group of bfm/plktlps revealed the key regulators in controlling biofilm of *B. licheniformis* by *L. plantarum*. Significant regulations in pathways of antibiotics biosynthesis and secondary metabolism biosynthesis help the biofilm cells to enhance their survival strategy by inhibiting the competitors. Up-regulation of serine protease is also related to interspecific competition. For example, the serine protease produced by *Staphylococcus epidermidis* may inhibits biofilm formation by *S. aureus* and even degrades *S. aureus* biofilms (Vandecandelaere, Depuydt, Nelis, & Coenye, 2014). On the other hand, serine levels are considered as an intracellular signal for biofilm activation of *B. subtilis*, because interference of converting serine to pyruvate led to a delay in biofilm formation (Greenwich et al., 2019). For bfm/plktlps, significant down-regulations of serine-protein kinase, phosphoserine aminotransferase, which are related to pyruvate metabolism, may have important function on biofilm control of *B. licheniformis*. Significant up-regulations of Spo0F and KapB, and significant down-regulations of MotB, FliG and FliK are only observed in bfm/plktlps, which may be the key targets for *L. plantarum* to affect biofilm by *B. licheniformis*. Results of biofilm intervention by *L. plantarum* reflected the important role of bacterial chemotaxis, flagellar assembly, and two-component system on biofilm formation of *B. licheniformis*. PPI network also revealed that two-component system pathway was not significantly detected in the bfm/plktlps comparison, in other words, *L. plantarum* metabolites cut off the bridge between biofilm-related pathways and primary metabolic pathways of *B. licheniformis*, becoming a probable cause of the biofilm inhibition.

5. Conclusions

In conclusion, TMT-based quantitative proteomics between biofilm cells and planktonic cells revealed the regulatory mechanisms of *B. licheniformis* biofilm formation and control. The processes of matrix production and sporulation are associated with each other. Bacterial chemotaxis, flagellar assembly, and two-component system played important roles on biofilm formation of *B. licheniformis*, and the proteins involved in those pathways are also key regulators for *L. plantarum* to interevent its biofilm formation. The proteomics analysis of biofilm formation provides theoretical basis for prospective strategies on biofilm control of *B. licheniformis*. Future studies are expected to determining the structure of specific anti-biofilm metabolites produced by *L. plantarum*, and thus providing novel and green biofilm control strategies.

CRediT author statement

Ni Wang: Conceptualization, Formal analysis, Data curation, Writing- Original draft preparation.
Faizan Ahmed Sadiq: Writing- Reviewing and Editing.
Shanshan Li: Software.
Guoqing He: Conceptualization, Supervision.
Lei Yuan: Conceptualization, Writing-Reviewing and Editing.

Acknowledgements

This study was supported by National Natural Science Foundation of China (No. 31772080), Chinese Institute of Food Science and Technology–Abbott Food Nutrition and Safety Special Scientific Research Fund (No. 2018–02).

Appendix A. Supplementary data

Supplementary data to this article can be found online at https://doi.org/10.1016/j.foodcont.2019.107029.

References

Ashburner, M., Ball, C. A., Blake, J. A., Botstein, D., Butler, H., Cherry, J. M., et al. (2000). Gene Ontology: Tool for the unification of biology. *Nature Genetics, 25*(1), 25–29.

Blair, K. M., Turner, L., Winkelman, J. T., Berg, H. C., & Kearns, D. B. (2008). A molecular clutch disables flagella in the *Bacillus subtilis* biofilm. *Science, 320*(5883), 1636–1638.

Bremer, P. J., Fillery, S., & McQuillan, A. J. (2006). Laboratory scale Clean-In-Place (CIP) studies on the effectiveness of different caustic and acid wash steps on the removal of dairy biofilms. *International Journal of Food Microbiology, 106*(3), 254–262.

Bridier, A., Briandet, R., Thomas, V., & Dubois-Brissonnet, F. (2011). Resistance of bacterial biofilms to disinfectants: A review. *Biofouling, 27*(9), 1017–1032.

Castro, J., Franca, A., Bradwell, K. R., Serrano, M. G., Jefferson, K. K., & Cerca, N. (2017). Comparative transcriptomic analysis of *Gardnerella vaginalis* biofilms vs. planktonic cultures using RNA-seq. *Npj Biofilms and Microbiomes, 3* UNSP 3.

Crielly, E. M., Logan, N. A., & Anderton, A. (1994). Studies on the *Bacillus flora* of milk and milk-products. *Journal of Applied Bacteriology, 77*(3), 256–263.

Cui, X., Chen, C., Liu, Y., Zhou, D., & Liu, M. (2019). Exogenous refractory protein enhances biofilm formation by altering the quorum sensing system: A potential hazard of soluble microbial proteins from WWTP effluent. *The Science of the Total Environment, 667*, 384–389.

Gao, T. T., Ding, M. Z., Yang, C. H., Fan, H. Y., Chai, Y. R., & Li, Y. (2019). The phosphotransferase system gene *ptsH* plays an important role in MnSOD production, biofilm formation, swarming motility, and root colonization in *Bacillus cereus* 905. *Research in Microbiology, 170*(2), 86–96.

Gao, T. T., Li, Y., Ding, M. Z., Chai, Y. R., & Wang, Q. (2017). The phosphotransferase system gene *ptsI* in *Bacillus cereus* regulates expression of *sodA2* and contributes to colonization of wheat roots. *Research in Microbiology, 168*(6), 524–535.

Greenwich, J., Reverdy, A., Gozzi, K., Di Cecco, G., Tashjian, T., Godoy-Carter, V., et al. (2019). A decrease in serine levels during growth transition triggers biofilm formation in *Bacillus subtilis*. *Journal of Bacteriology, 201*(15) e00155-19.

Huang, Y. Y., Morvay, A. A., Shi, X. M., Suo, Y. J., Shi, C. L., & Knothel, S. (2018). Comparison of oxidative stress response and biofilm formation of *Listeria monocytogenes* serotypes 4b and 1/2a. *Food Control, 85*, 416–422.

Hudson, K. D., Corfe, B. M., Kemp, E. H., Feavers, I. M., Coote, P. J., & Moir, A. (2001). Localization of GerAA and GerAC germination proteins in the *Bacillus subtilis* spore. *Journal of Bacteriology, 183*(14), 4317–4322.

Kanehisa, M., Goto, S., Sato, Y., Furumichi, M., & Tanabe, M. (2012). KEGG for integration and interpretation of large-scale molecular data sets. *Nucleic Acids Research, 40*(D1), D109–D114.

Karathanasi, G., Bojer, M. S., Baldry, M., Johannessen, B. A., Wolff, S., Greco, I., et al. (2018). Linear peptidomimetics as potent antagonists of *Staphylococcus aureus* agr quorum sensing. *Scientific Reports, 8*, 3562.

Liu, T. J., Li, Y., Chen, J. C., Sadiq, F. A., Zhang, G. H., Li, Y., et al. (2016). Prevalence and diversity of lactic acid bacteria in Chinese traditional sourdough revealed by culture dependent and pyrosequencing approaches. *Lwt-Food Science and Technology, 68*, 91–97.

Maddela, N. R., Sheng, B., Yuan, S., Zhou, Z., Villamar-Torres, R., & Meng, F. (2019). Roles of quorum sensing in biological wastewater treatment: A critical review. *Chemosphere, 221*, 616–629.

Maes, S., Heyndrickx, M., Vackier, T., Steenackers, H., Verplaetse, A., & De Reu, K. (2019). Identification and Spoilage Potential of the remaining dominant microbiota on food contact surfaces after cleaning and disinfection in different food industries. *Journal of Food Protection, 82*(2), 262–275.

Merino, L., Trejo, F. M., De Antoni, G., & Golowczyc, M. A. (2019). *Lactobacillus* strains inhibit biofilm formation of *Salmonella* sp. isolates from poultry. *Food Research International, 123*, 258–265.

Reginensi, S. M., Gonzalez, M. J., Olivera, J. A., Sosa, M., Juliano, P., & Bermudez, J. (2011). RAPD-based screening for spore-forming bacterial populations in Uruguayan commercial powdered milk. *International Journal of Food Microbiology, 148*(1), 36–41.

Ren, D. C., Bedzyk, L. A., Setlow, P., Thomas, S. M., Ye, R. W., & Wood, T. K. (2004). Gene expression in *Bacillus subtilis* surface biofilms with and without sporulation and the importance of *yveR* for biofilm maintenance. *Biotechnology and Bioengineering, 86*(3), 344–364.

Rey, M. W., Ramaiya, P., Nelson, B. A., Brody-Karpin, S. D., Zaretsky, E. J., Tang, M., et al. (2004). Complete genome sequence of the industrial bacterium *Bacillus licheniformis* and comparisons with closely related *Bacillus species*. *Genome Biology, 5*(10), R77.

Ruckert, A., Ronimus, R. S., & Morgan, H. W. (2004). A RAPD-based survey of thermophilic bacilli in milk powders from different countries. *International Journal of Food Microbiology, 96*(3), 263–272.

Sadiq, F. A., Flint, S., Yuan, L., Li, Y., Liu, T. J., & He, G. Q. (2017). Propensity for biofilm formation by aerobic mesophilic and thermophilic spore forming bacteria isolated from Chinese milk powders. *International Journal of Food Microbiology, 262*, 89–98.

Sadiq, F. A., Li, Y., Liu, T. J., Flint, S., Zhang, G. H., & He, G. Q. (2016b). A RAPD based study revealing a previously unreported wide range of mesophilic and thermophilic spore formers associated with milk powders in China. *International Journal of Food Microbiology, 217*, 200–208.

Sadiq, F. A., Li, Y., Liu, T., Flint, S., Zhang, G., Yuan, L., et al. (2016a). The heat resistance and spoilage potential of aerobic mesophilic and thermophilic spore forming bacteria isolated from Chinese milk powders. *International Journal of Food Microbiology, 238*, 193–201.

Sarjit, A., & Dykes, G. A. (2017). Antimicrobial activity of trisodium phosphate and sodium hypochlorite against *Salmonella* biofilms on abiotic surfaces with and without soiling with chicken juice. *Food Control, 73*, 1016–1022.

Subramaniam, A. R., DeLoughery, A., Bradshaw, N., Chen, Y., O'Shea, E., Losick, R., et al. (2013). A serine sensor for multicellularity in a bacterium. *Elife, 2*, e01501.

Subramanian, S., Gao, X. H., Dann, C. E., & Kearns, D. B. (2017). MotI (DgrA) acts as a molecular clutch on the flagellar stator protein MotA in *Bacillus subtilis*. *Proceedings of the National Academy of Sciences of the United States of America, 114*(51), 13537–13542.

Suriyanarayanan, T., Lin, Q. S., Kwang, L. T., Mun, L. Y., Truong, T., & Seneviratne, C. J. (2018). Quantitative proteomics of strong and weak biofilm formers of *Enterococcus faecalis* reveals novel regulators of biofilm formation. *Molecular & Cellular Proteomics, 17*(4), 643–654.

Toyofuku, M., Nomura, N., Kuno, E., Tashiro, Y., Nakajima, T., & Uchiyama, I. (2008). Influence of the *Pseudomonas* Quinolone signal on denitrification in *Pseudomonas aeruginosa*. *Journal of Bacteriology, 190*(24), 7947–7956.

Tyanova, S., Temu, T., Sinitcyn, P., Carlson, A., Hein, M. Y., Geiger, T., et al. (2016). The Perseus computational platform for comprehensive analysis of (prote)omics data. *Nature Methods, 13*(9), 731–740.

Vandecandelaere, I., Depuydt, P., Nelis, H. J., & Coenye, T. (2014). Protease production by *Staphylococcus epidermidis* and its effect on *Staphylococcus aureus* biofilms. *Pathogens and Disease, 70*(3), 321–331.

Vasquez, J., Tal-Gan, Y., Cornilescu, G., Tyler, K. A., & Blackwell, H. (2017). Simplified AIP-II peptidomimetics are potent inhibitors of *Staphylococcus aureus* AgrC quorum sensing receptors. *ChemBioChem, 18*(4), 413–423.

Vlamakis, H., Chai, Y. R., Beauregard, P., Losick, R., & Kolter, R. (2013). Sticking together: Building a biofilm the Bacillus subtilis way. *Nature Reviews Microbiology, 11*(3), 157–168.

Voigt, B., Schweder, T., Sibbald, M., Albrecht, D., Ehrenreich, A., Bernhardt, J., et al. (2006). The extracellular proteome of *Bacillus licheniformis* grown in different media and under different nutrient starvation conditions. *Proteomics, 6*(1), 268–281.

Wang, Y., Yi, L., Zhang, J., Sun, L., Wen, W., Zhang, C., et al. (2018). Functional analysis of superoxide dismutase of *Salmonella typhimurium* in serum resistance and biofilm formation. *Journal of Applied Microbiology, 125*(5), 1526–1533.

Wang, N., Yuan, L., Sadiq, F. A., & He, G. Q. (2019). Inhibitory effect of *Lactobacillus plantarum* metabolites against biofilm formation by *Bacillus licheniformis* isolated from milk powder products. *Food Control, 106* UNSP 106721.

Ward, E., Kim, E. A., Panushka, J., Botelho, T., Meyer, T., Kearns, D. B., et al. (2019). Organization of the flagellar switch complex of *Bacillus subtilis*. *Journal of Bacteriology, 201*(8), e00626.

Wasfi, R., Abd El-Rahman, O. A., Zafer, M. M., & Ashour, H. M. (2018). Probiotic *Lactobacillus* sp inhibit growth, biofilm formation and gene expression of caries-inducing *Streptococcus mutans*. *Journal of Cellular and Molecular Medicine, 22*(3), 1972–1983.

Wisniewski, J. R., Zougman, A., Nagaraj, N., & Mann, M. (2009). Universal sample preparation method for proteome analysis. *Nature Methods, 6*(5) 359-U60.

Yang, X. Q., Wang, H., He, A. N., & Tran, F. (2018). Biofilm formation and susceptibility to biocides of recurring and transient *Escherichia coli* isolated from meat fabrication equipment. *Food Control, 90*, 205–211.

Yin, L., Li, Q., Xue, M., Wang, Z., Tu, J., Song, X., et al. (2019). The role of the *phoP* transcriptional regulator on biofilm formation of avian pathogenic *Escherichia Coli. Avian pathology. Journal of the W.V.P.A,* 1–23.

Yuan, L., Hansen, M. F., Roder, H. L., Wang, N., Burmolle, M., & He, G. (2019). Mixed-species biofilms in the food industry: Current knowledge and novel control strategies. *Critical Reviews in Food Science and Nutrition*. https://doi.org/10.1080/10408398.2019.1632790.

Yuan, L., Sadiq, F. A., Burmolle, M., Liu, T. J., & He, G. Q. (2018). Insights into bacterial milk spoilage with particular emphasis on the roles of heat-stable enzymes, biofilms, and quorum sensing. *Journal of Food Protection, 81*(10), 1651–1660.

Zheng, Y. J., Li, Y. M., Long, H. Y., Zhao, X. J., Jia, K. K., Li, J., et al. (2018). *bifA* regulates biofilm development of *Pseudomonas putida* MnB1 as a Primary Response to H_2O_2 and Mn^{2+}. *Frontiers in Microbiology, 9*, 1490.

Zou, M. M., & Liu, D. H. (2018). A systematic characterization of the distribution, biofilm-forming potential and the resistance of the biofilms to the CIP processes of the bacteria in a milk powder processing factory. *Food Research International, 113*, 316–326.